Available online at www.sciencedirect.com
SCIENCE DIRECT®
International Journal of Heat and Mass Transfer 47 (2004) 4967–4977
International Journal of HEAT and MASS TRANSFER
www.elsevier.com/locate/ijhmt

A numerically-based parametric study of heat transfer off an inclined surface subject to impinging airflow

Srinivasan C. Rasipuram, Karim J. Nasr *

Department of Mechanical Engineering, Kettering University, 1700 West Third Avenue Flint, MI 48505, United States

Received 9 January 2004; received in revised form 25 June 2004
Available online 23 August 2004

Abstract

Impinging jets may be used to achieve enhanced local heat transfer for convective heating, cooling, or drying. The issuing jet may contact the surface normally or obliquely. Factors such as jet attachment, surface angle, jet angle and size, separation distance between jet orifice and surface of impingement, and trajectory influence heat transfer dramatically. This study addresses the thermal problem of jet impingement on an inclined surface and is motivated by the practical application of air jets issuing out of a defroster's nozzles and impinging on the inclined windshield surface of a vehicle. The effects of incoming fluid velocity, openings' geometry (circular vs. rectangular), number of openings, angle that the inclined surface makes with the horizontal plane and angle of impinging jet on heat transfer are examined. Fluid mechanics and heat transfer characteristics are exhibited in details for a configuration with three rectangular openings. A comparative study for other configurations is also featured. The results are correlated in terms of governing dimensionless parameters through numerically-based correlations that are useful for predicting heat transfer on an inclined surface subject to impinging airflow.

Keywords: Impinging jets; Inclined surfaces; Heat transfer coefficient

1. Introduction

Impinging jets are an established method for obtaining high local heat transfer coefficients between a fluid and a surface. Applications include tempering of glass plates, annealing of metal sheets, drying of textile and paper products, cooling of electronic components, cooling of heated components in gas turbine engines, deicing and defogging of automotive windshields, to name a few. In such applications, the temperature distribution resulting from the jet interaction with the inclined surface, the effect of the jet angle, inclined surface angle, opening geometry, and number of openings are critical design factors.

In the current study, the specific application of interest is air issuing from the defroster's nozzles of a vehicle and impinging on a glass windshield. The performance of the defroster's flow affects its effectiveness in defrosting ice on the external surface and removing fog internally. In lieu of ad hoc testing, various factors can be examined for optimizing system's performance numerically. Relying on advances in numerical modeling and utilizing Computational Fluid Dynamics (CFD) tools,

* Corresponding author. Tel.: +1 810 762 7876; fax: +1 810 762 7860.
E-mail address: knasr@kettering.edu (K.J. Nasr).

0017-9310/$ - see front matter © 2004 Elsevier Ltd. All rights reserved.
doi:10.1016/j.ijheatmasstransfer.2004.06.030

Nomenclature

A	total area of the surface	T	temperature
h	heat transfer coefficient	U	solution vector
D	hydraulic diameter of one opening		
H	vertical height from the center of the nozzle exit to the inclined surface	*Greek symbols*	
		β	jet angle in the YZ plane
H_1	width of the inclined surface	ϵ	convergence criterion
k	turbulent kinetic energy	ε	dissipation rate of turbulent kinetic energy
Re	Reynolds number based on H_1	ϕ	jet angle in the XY plane
Nu	Nusselt number based on H_1	θ	surface inclination angle

a designer can predict the performance of a system and optimize its objectives cost-effectively.

The purpose of this study is to document heat transfer between an inclined surface and a flow of air impinging on it. Various configurations are investigated. The paper leads with a validation case comparing numerically-computed local surface temperatures to experimentally-measured values. It then presents a detailed study case of three rectangular openings accounting for airflow impingement angles in the XY plane (φ) and YZ plane (β) and for various inclined surface angles. The paper then addresses other configurations varying the number and geometry of openings. Fig. 1 presents a general schematic of the model, showing two rectangular openings. The external geometry is the same in all cases. However, effects of the angle of the inclined surface, number and position of the openings serving as inlets to the computational domain, angle of the incoming fluid, and fluid velocity on heat transfer are studied. Fig. 2 illustrate the orientations of the jet in the XY and YZ planes and the vertical distance from the center of the opening to the inclined surface. Fig. 3 shows the position of the rear outlets and associated dimensions. Figs. 4 and 5 illustrate inlet configurations with one, two and three rectangular openings and two circular openings. The outlet configuration is common for all cases. In addition to presenting the fluid mechanics of this problem, the detailed study case of three rectangular openings aims at studying the effect of various inclined surface angles ($\theta = 30°$, 40°, and 50°), the effect of the jet angle in the XY plane ($\phi = 30$–$90°$ in increments of 10°), and the effect of jet angle in the YZ plane

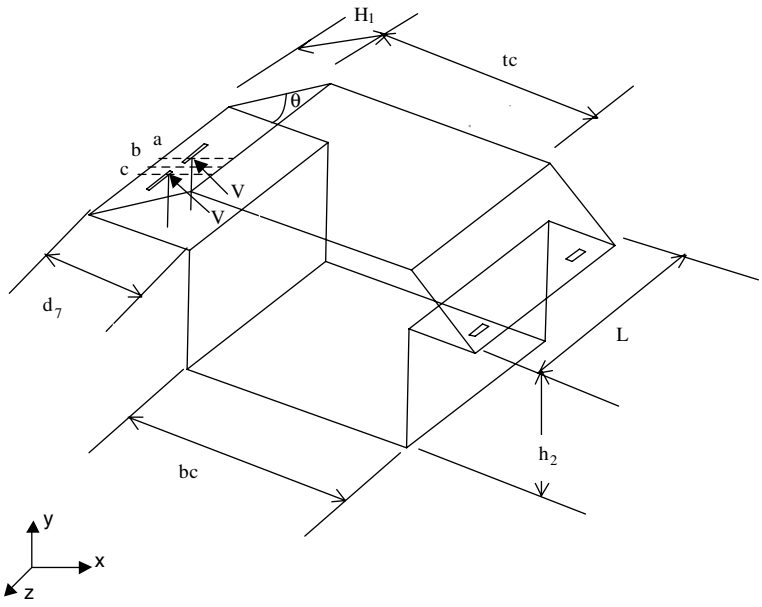

Fig. 1. General schematic of the model with two rectangular openings.

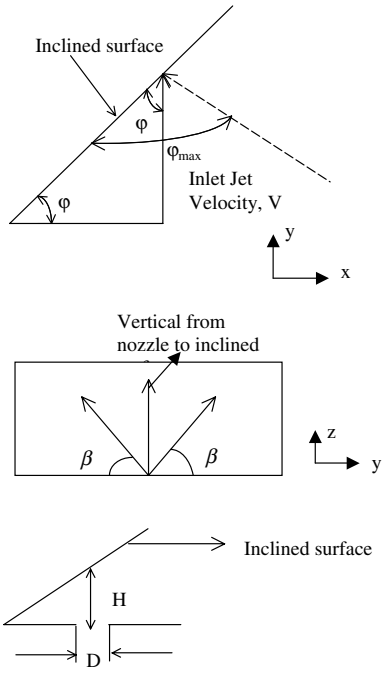

Fig. 2. A graphical representation of different orientations of the jet and H/D.

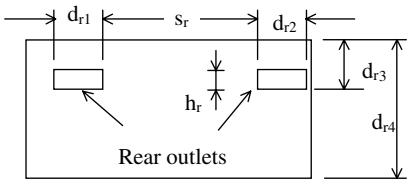

Distance between outlets - rear, s_r	0.891 m
Width of rear dash board, d_{r4}	0.45 m
Width of outlet - rear, d_{r1}, d_{r2}	0.141 m
Length of outlet - rear, h_r	0.039 m
Location of outlet - rear, d_{r3}	0.140 m

Fig. 3. Rear outlets and related dimensions.

(β = 35–85° in increments of 10° and also for 90°) on heat transfer. The comparative study comparing one, two, and three rectangular openings and two circular openings accounts for the variation of the jet angle in the XY plane (ϕ) between 30° and 90° but for a fixed inclined surface angle (θ) of 30° and a fixed jet angle in the YZ plane (β) of 90°.

It is worth noting that this study is not restricted to the windshield scenario but can also be applicable to the thermal problem of jets impinging on an inclined surface. The paper concludes with numerically-based correlations which are useful for predicting heat transfer for air impinging of an inclined surface.

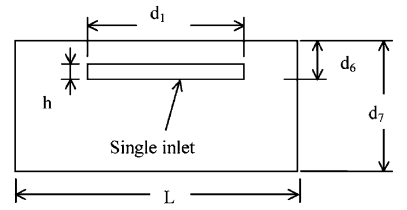

Length of inclined surface, L	1.447 m
Width of nozzle exit plane, d_1	0.482 m
Length of nozzle exit plane, h	0.038 m
Width of dash board, d_7	0.685 m
Location of nozzle, d_6	0.153 m

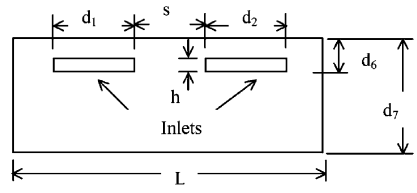

Length of inclined surface, L	1.447 m
Width of nozzle exit plane, d_1, d_2	0.241 m
Distance between nozzle exit planes, s	0.127 m
Length of nozzle exit plane, h	0.019 m
Width of dash board, d_7	0.685 m
Location of nozzle, d_6	0.134 m

Fig. 4. Inlets representation for: (a) one and (b) two rectangular openings.

2. Literature review

The literature has ample references on impinging jets and thus a number of investigators found it useful to summarize gathered knowledge [1–4]. Studies of close relevance to current investigations are revisited here. In addressing heat/mass transfer of an oblique jet, Sparrow and Lovell [5] observed that the point of maximum mass transfer was displaced from the geometric impingement point, with the extent of the displacement increasing with greater jet inclination for an obliquely impinging circular jet on a surface. Goldstein and Franchett [6] conducted experiments on a flat surface subject to an oblique impinging jet and indicated a displacement of the peak heat transfer from the geometric center of the jet origin, the displacement being a function primarily of impingement angle. Mohanty and Tawfek [7] carried out heat transfer measurements from an isothermal plate due to an impinging air jet. Heat transfer was reported to decay exponentially with radial distance from the highest value at the impingement point. Lee et al. [8] measured local heat transfer for a turbulent submerged air jet issuing, normal to a heated flat plate, from an elliptical nozzle. For some

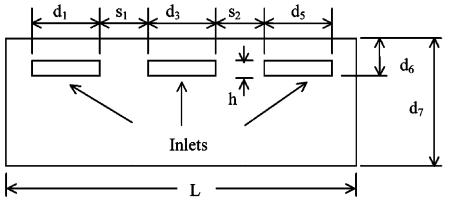

Length of inclined surface, L	1.447 m
Width of nozzle exit plane, d_1, d_3, d_5	0.161 m
Distance between nozzle exit planes, s_1, s_2	0.161 m
Length of nozzle exit plane, h	0.013 m
Width of dash board, d_7	0.685 m
Location of nozzle, d_6	0.128 m

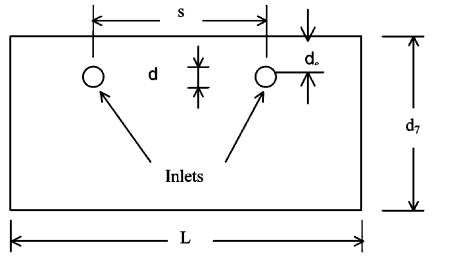

Length of inclined surface, L	1.447 m
Distance between nozzle exit planes, s	0.368 m
Length of nozzle exit plane, d	0.035 m
Width of dash board, d_7	0.685 m
Location of nozzle, d_6	0.125 m

Fig. 5. Inlets representation for: (a) three rectangular and (b) two circular openings.

configurations, the investigators noted second and third maxima for Nusselt numbers. Huang and El-Genk [9] investigated heat transfer between a uniformly heated flat plate and an impinging circular air jet experimentally, particularly for small values of Reynolds number (6000–60,000) and jet spacing, producing a heat transfer correlation. Bernard et al. [10] used different experimental techniques to describe the flow pattern generated by fifteen jets impinging on a plane wall. Laser sheet visualizations were reported to show complex vortical structures such as the ground vortex and secondary rolling-ups near the target plate. Bailey and Bunker [11] used liquid crystals to measure heat transfer coefficients due to dense and sparse jet arrays. They reported close agreement with the results of other investigators for similar geometries and flow conditions. Roy et al. [12] conducted an experimental and numerical study of heat transfer off an inclined surface subject to a pair of rectangular air jets impinging on the inclined surface. The authors validated the numerical results with experimental data, compared the predicted local and average heat transfer coefficients to the experimental results and studied the effect of three different turbulence intensity levels. Roy and Patel [13] studied the dominant fluid-thermal characteristics of a pair of rectangular air jets impinging on an inclined surface. Local and average Nusselt numbers were evaluated with two different boundary conditions on three specified lines located on the inclined surface. The authors presented a correlation between stagnation Nusselt number and Reynolds number and reported the effect of jet impingement angle on local and average Nusselt number. Finally, the authors documented a correlation between average Nusselt number, Reynolds number and jet angle.

It is worth noting here the difference between [13] and current investigations. Studies by Roy and Patel [13] dealt with two rectangular openings whereas the current paper deals with one, two and three rectangular openings and two circular openings. The significance of this investigation is to study the heat transfer patterns on the inclined surface as a result of jets issuing from different configurations (one, two and three rectangular openings, and two circular openings) and to decide on the configuration that yields the maximum overall heat transfer off the inclined surface. The current study also documents correlations of Nusselt number as a function of Reynolds number and φ for each configuration. In addition, the numerical correlation provided here for the detailed study case, with three rectangular openings, addresses additional jet angles (φ and β) affecting heat transfer and presents Nu as a power function of Re, (H/D) or θ, φ and β.

3. Computational modeling

This computational study was carried out using *Fluent* [14], a finite-volume code. The RNG based $k-\varepsilon$ turbulence model was utilized for simulations. The use of this turbulence model was based on having provided good correlation with the experimental results when used in earlier studies [12]. Details of the numerical model are consistent with what was used in earlier studies [12,13] and need not be repeated here. The solution was declared convergent when the maximum residual for each of the state variables was smaller than a convergence criterion of ϵ. The convergence of a solution vector U on node n is defined as the norm

$$\frac{\|U_n - U_{n-1}\|}{\|U_n\|} \leqslant \epsilon$$

Convergence criteria selected for the governing equations are 10^{-3} for continuity, momentum, k, and ε and 10^{-6} for the energy equation. This convergence criterion was selected as numerical simulations with these criteria matched experimental results [12] and as demonstrated for the validation case in the next section.

3.1. Boundary conditions

All walls were considered as adiabatic, except the inclined surface being subject to an applied heat flux of 350 W/m^2. Uniform air velocity (ranging from 5 to 30 m/s) at 293 K exits the openings and impinges on the inclined surface. A turbulence intensity of 10% was used at the inlet. Reynolds number was varied from 2.71×10^5 to 1.62×10^6 where the width of the inclined surface ($H_1 = 0.791$ m) has been considered as a characteristic length. For multiple openings, air with the same velocity exits out of each opening. The outlets have been considered as pressure outlets with a zero gauge pressure (exiting to the ambient). A no-slip boundary condition is enforced at all walls. The shear stress and heat transfer between the fluid and wall are computed based on the flow details in the local flow field. Standard wall functions used in this numerical study are based on those found in Launder and Spalding [15]. Wall-functions are a collection of semi-empirical formulas that in effect bridge the viscosity-affected region between the wall and the fully turbulent region. The wall function approach is used because of its robustness and reasonable accuracy. The pressure–velocity linking and the convection-diffusion terms linking are achieved by the SIMPLE algorithm. More information on this algorithm can be found in the Fluent [14] user manual.

3.2. Effect of grid size on surface temperatures

The geometry and volume mesh were generated in Gambit [16]. The computational domain was discretized into tetrahedral finite volumes. Analysis was performed on the data to investigate the effect of surface temperature T_s on the heat transfer coefficient, h and to decide on the accuracy required for grid independence studies. A surface temperature (T_s) of 310 K is considered as a reference temperature with a heat flux of 350 W/m^2 and an incoming air temperature (T_∞) of 293 K.

A change of ±1 K from a T_s of 310 K results in approximately 5% change in h. Therefore, an optimal grid size is selected if temperature changes between subsequent grid sizes are within 1 K. The grid size was increased from 100,000 cells in increments of 50,000 cells until the change in T_s with successive grid sizes is within 1 K at eight points (p_1–p_8), as shown in Fig. 6 at a y of 0.2 m. The points p_1 to p_8 on the inclined surface along L are located at $z = 1.247$, 1.147, 1.0, 0.8, 0.6, 0.45, 0.3, and 0.2 m; respectively. This effect of grid size is for the detailed study case of three rectangular openings, with 30° inclined surface angle ($\theta = 30$), $Re = 5.42 \times 10^5$, $\varphi = 60°$ and $\beta = 90°$. Similar studies have been conducted for all other configurations. When comparing grid sizes of 352,508 cells and 300,645 cells, the maximum temperature change along the eight points in the case presented is 0.41 K. Therefore, for this case,

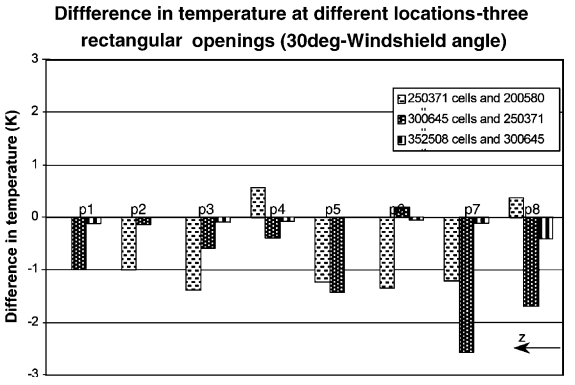

Fig. 6. Difference in temperature at locations p_1 to p_8 for different grid sizes ($\theta = 30°$, $\phi = 60°$ and $\beta = 90°$).

the grid with 300,645 cells was decided on for further simulations.

4. Simulation results validation

In an earlier study [12], local surface temperatures were measured and reported. The experimental set-up involved heating the middle section of the inclined surface via a centrally located heating pad. The imposed heat flux was measured to be 368 W/m^2 on the heated section of the external surface. Details of the experimental layout have been described fully in [12]. The experimentally-based data is used as a validation case for current simulations. Therefore, a numerical simulation was constructed to match the experimental set-up exactly. As a result, local surface temperatures were extracted and compared. The inside of the inclined surface was subject to air flow. Fig. 7 presents a comparison between the experimentally-based temperature contours and the simulation-produced temperature contours. Examining both contours, the numerical simulation correlates reasonably well with the experimental results. Also, the experimentally-based average heat transfer coefficient was reported to be 29.4 W/m^{2}K [12] compared to a simulation-based value of 26.3 W/m^{2}K for this validation case.

5. Detailed study case for three rectangular openings

Upon validation of the numerical simulation, a detailed study was carried out for three rectangular openings. The entire inclined surface is subject to an imposed heat flux of 350 W/m^2. Fig. 8 illustrates the issuing jet flow and describes how each jet creates a pair of counter rotating vortices in the crosswise direction. The jet spreads more due to these bound vortices, covering a larger cross-section. This is the result of the bound

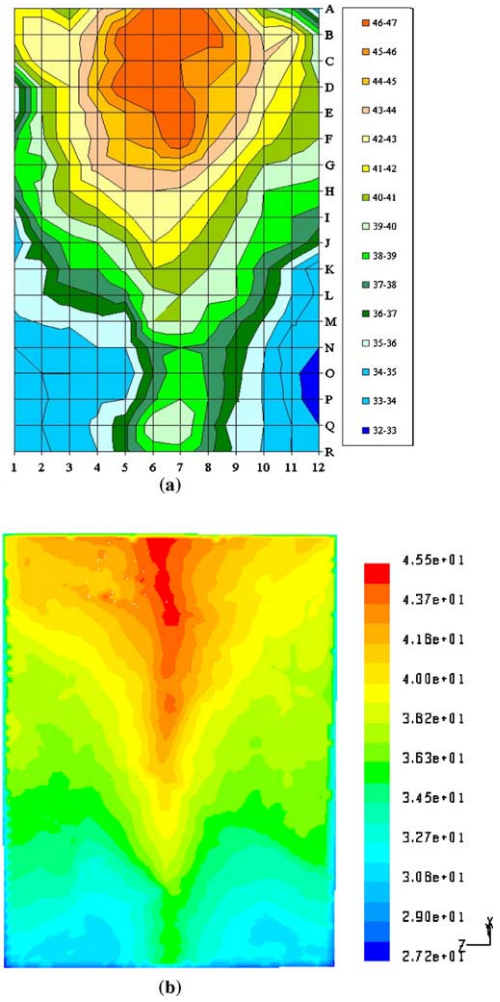

Fig. 7. Temperature contours beneath a heated section on the inclined surface: (a) contours measured experimentally [12] and (b) contours from simulations.

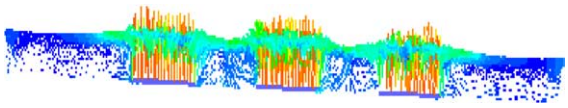

Fig. 8. Velocity vectors at the inlets demonstrating counter rotating vortices—$Re = 1.62 \times 10^6$, $\theta = 30°$, $\varphi = 60°$, $\beta = 90°$.

vortices being confined in a smaller space, inducing larger crosswise components of velocity and thus aiding the spread of the jet. The flow emerging from the openings is subjected to bending due to the impingement, thus reducing the effect of boundary layer thickness significantly.

To further illustrate the effect of the jet angle (β) on heat transfer between the inclined surface and the impinging air, simulation runs were carried out for air issuing from the center opening at $\beta = 90°$ and from the two neighboring openings at $\beta = 75°$. This is done for $Re = 1.62 \times 10^6$, $\theta = 30°$, and $\varphi = 60°$. Fig. 9 displays velocity vectors along various planes through the computational domain, while Fig. 10 shows pathlines for the impinging airflow. Each jet creates a stagnation zone about the impingement location, and then spreads in all directions across the surface. Fig. 11 shows the velocity vectors in the XY plane along $z = 1.0450$ m cut through one of the openings (inlet). It shows flow impingement and redirection along the inclined surface as well as

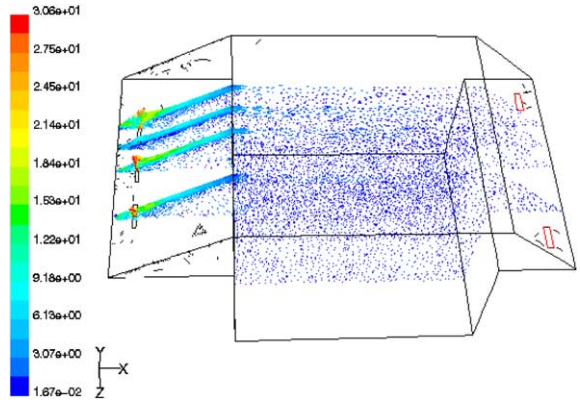

Fig. 9. Flow vectors along planes $z = 0.4020$, $z = 0.5628$, $z = 0.7235$, and $z = 1.0450$ m.

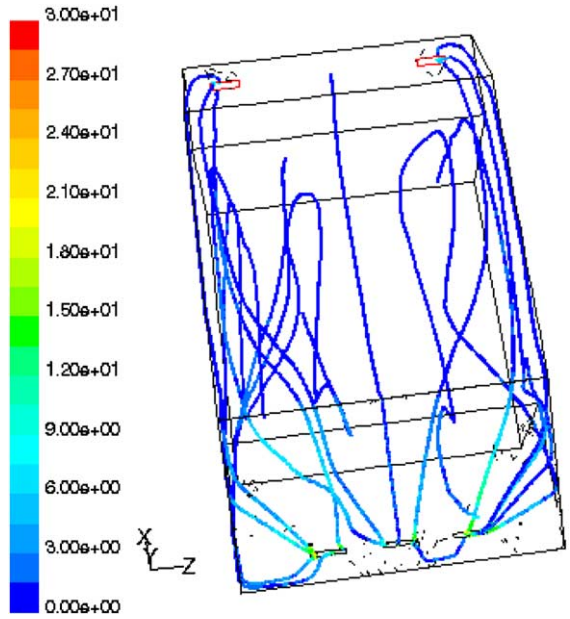

Fig. 10. Particles tracking through pathlines for the impinging flow.

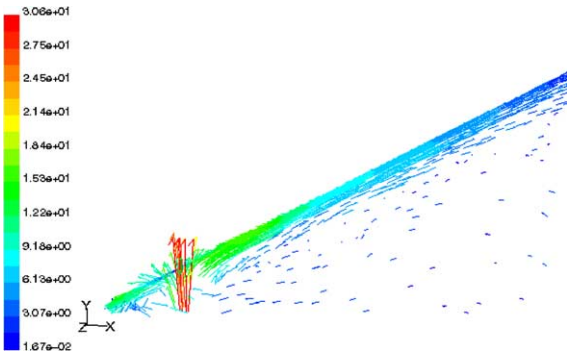

Fig. 11. Velocity vectors in XY plane cut at an inlet along $z = 1.045$ m.

towards the corner between the inclined surface and the horizontal plane. The jet impinging on the inclined surface and the path of air after impingement can be clearly seen. Within the stagnation zone, flow is influenced by the target surface and is decelerated and accelerated in the normal (y) and transverse (z) directions. However, since the flow continues to entrain zero momentum fluid from the surroundings, horizontal acceleration cannot continue indefinitely and accelerating flow in the stagnation zone is transformed to a decelerating wall jet. The velocity of the jet after impingement increases in the wall jet region after a region of low velocity. The deflected jet, which becomes parallel to the impingement surface, behaves similarly to a radial wall jet in the fluid layer near the impingement wall. Once the flow detaches from the inclined surface and flows through the computational domain, it experiences recirculation. Further insights into the fluid mechanics within the computational domain can be gained by examining Fig. 12 and demonstrating recirculation. It is worth noting that recirculation characteristics can be weak or strong depending on the flow origin and whether it had originated from an inlet or a result of an interaction and entrainment. Fig. 13 reports a ground vortex near the

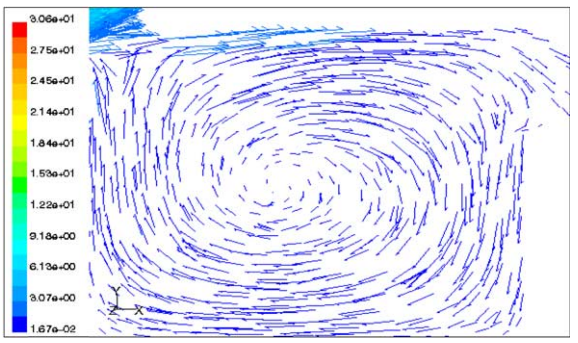

Fig. 12. Velocity vectors along $z = 1.045$ m demonstrating recirculation.

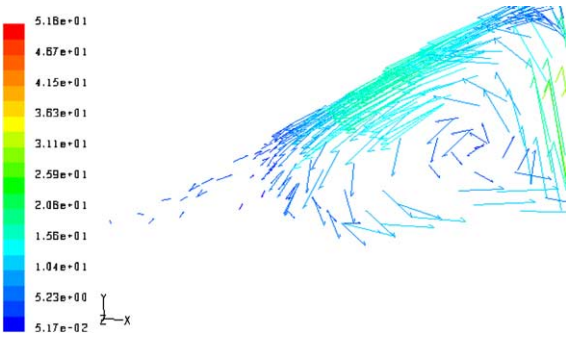

Fig. 13. Enlarges velocity vectors in the pocket region near the corner ($z = 0.7235$ m).

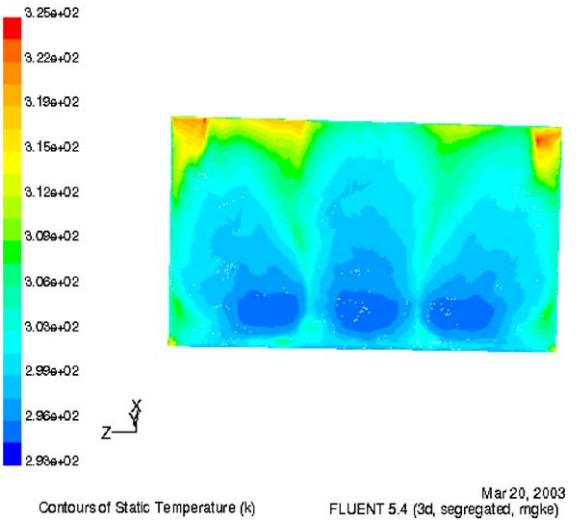

Fig. 14. Temperature contours on the inclined surface.

jet as seen in a similar application by Bernard et al. [10] as an enlarged view of the region between the impingement area and the corner. Fig. 14 displays the temperature contours and indicates that the lowest temperature is at the stagnation region where the jet impinges upon the inclined surface. Heat transfer decreases as the flow moves upward along the inclined surface from the point of impingement and as the boundary layer thickness increases. Below the jet impingement area, local temperatures are higher than those in the impingement zone. This is due to the inclination of the surface and that most of the fluid after impingement moves upward resulting in lower temperatures around and above the jet impingement point. As the area downstream of the jet impingement point sees lesser amount of fluid, the heat transfer is low resulting in higher temperatures. This is illustrated further in Fig. 15 showing the variation of the heat transfer coefficient

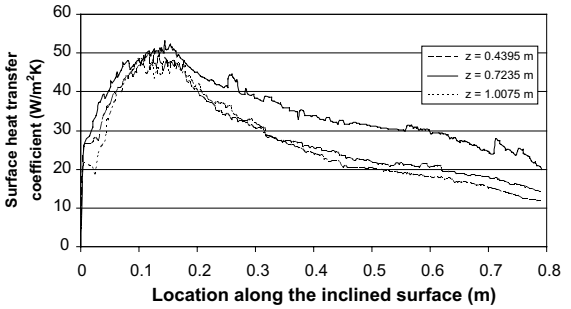

Fig. 15. Local heat transfer coefficients along lines a, b and c on the inclined surface.

along three planes (lines a, b, and c shown in Fig. 1). Similar variations are obtained along other planes.

6. Comparative results for different configurations

For comparing various configurations and the effect of number of openings, a comparative study was carried out for an applied heat flux of 350 W/m^2 on the inclined surface. All configurations are subject to the same boundary conditions and differ only in the number of openings and total inlet mass flow rates. The total hydraulic diameter (sum of individual hydraulic diameters) is the same for all configurations and is equivalent to 0.0705 m. The inlet velocity for the comparative study is 30 m/s ($Re = 1.62 \times 10^6$). The mass flow rate is 0.143 kg/s for one rectangular opening, 0.0716 kg/s for two rectangular and circular openings, and 0.0477 kg/s for three rectangular openings. When compared to the one rectangular opening configuration, the two rectangular and circular openings configurations experience 50% less flow and the three rectangular openings configuration experiences 67% less flow. Fig. 16 reports the computed local surface heat transfer coefficients on the inclined surface. The configuration with one rectangular opening (Fig. 16(a)) has more regions that represent high heat transfer areas compared to the other configurations. Temperature gradients on the inclined surface are very high in the case of two circular openings (Fig. 16(d)) as compared to other configurations. Fig. 17 compares local heat transfer coefficients for different configurations along the point of impingement, across the length of the inclined surface, L. All data plotted in Fig. 17 are for $Re = 1.62 \times 10^6$, $\theta = 30°$, $\varphi = 70°$. The indicated peaks correspond to the number of openings for the configuration. The configuration with two circular openings has relatively lesser spread compared to the configurations with rectangular openings, which results in a substantially lower average surface heat transfer coefficient value. Computing average heat transfer coefficients for

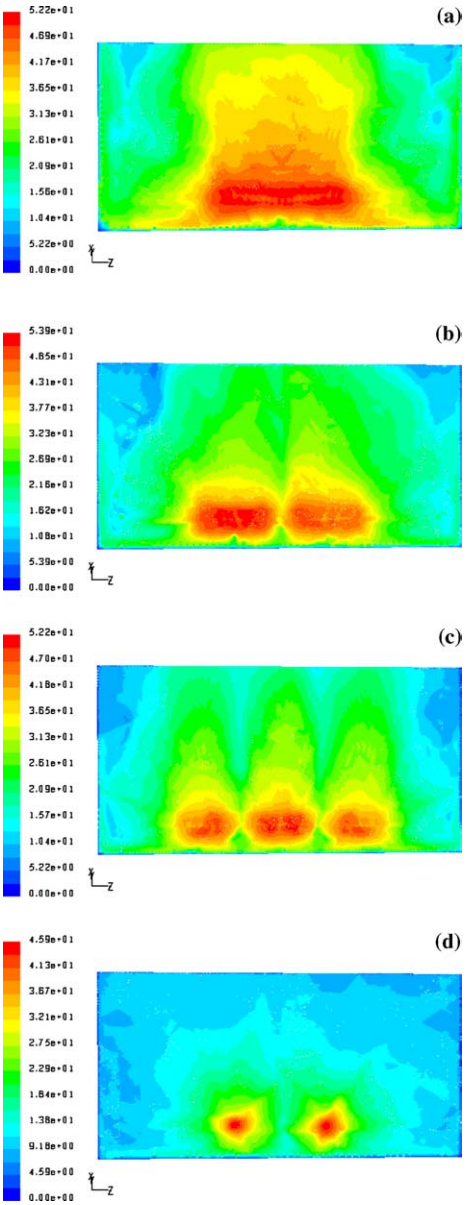

Fig. 16. Local heat transfer coefficient contours mapped onto the inclined surface for different configurations—$Re = 1.62 \times 10^6$, $\theta = 30°$, $\varphi = 70°$: (a) one rectangular opening; (b) two rectangular openings (c) three rectangular openings and (d) two circular openings.

each configuration resulted in the following values: 29.75, 25.07, and 23.59 W/m^{2}K for one, two and three rectangular openings; respectively, and 13.46 W/m^{2}K for two circular openings. Examining the peaks of Fig. 17, the maximum surface heat transfer value for all the configurations with rectangular openings is almost the same (51.02, 54.08, and 50.48 W/m^{2}K for one, two and three rectangular openings), whereas the configura-

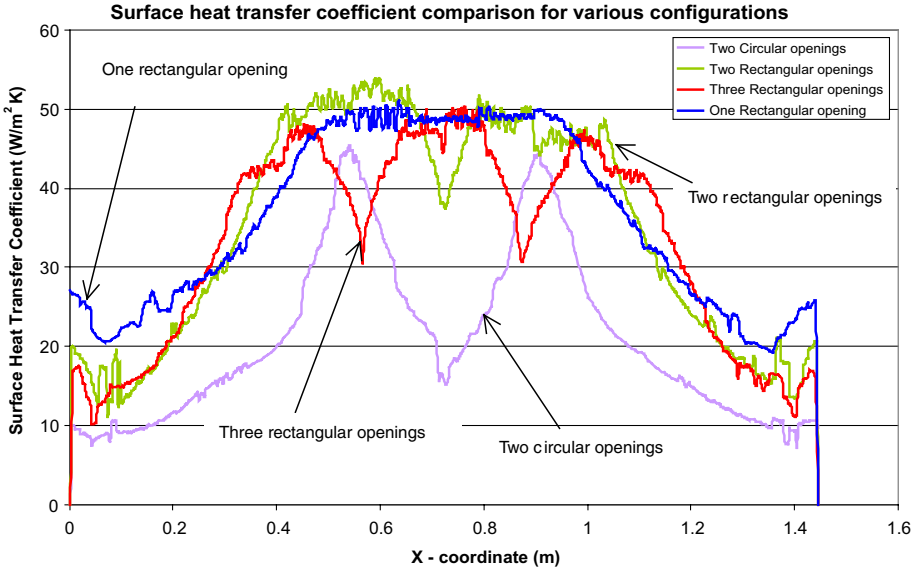

Fig. 17. Comparison of local heat transfer coefficients for different configurations along the point of impingement across L—$Re = 1.62 \times 10^6$, $\theta = 30°$, $\varphi = 70°$.

tion with two circular openings has a maximum surface heat transfer coefficient of 45.43 W/m^{2}K.

7. Curve fit correlations for various configurations

A number of variables affect heat transfer between the inclined surface that is subject to an imposed heat flux and the impinging airflow. Comparing all configurations and generating correlations for the purpose of predicting overall heat transfer was performed using average heat transfer coefficients. An area-weighted average of surface heat transfer coefficient is calculated for each case and used for scaling. The area-weighted average of a quantity is computed in Fluent by dividing the summation of the product of the selected field variable and facet area by the total area of the surface:

$$\frac{1}{A}\int h\,\mathrm{d}A = \frac{1}{A}\sum_{i=1}^{n} h_i|A_i|$$

A sample set of computed heat transfer coefficients is shown in Table 1. The complete data set can be found in [17]. The overall heat transfer coefficient off the inclined surface for the configuration with one rectangular opening was 20% more than that for the configuration with two rectangular openings, 25% more than that with three rectangular openings and 120% more than that with two circular openings.

For the comparative study, one hundred and eighty six simulations were performed covering a range of Reynolds numbers and issuing jet angles of the various configurations. The method of least squares was used to develop a correlation that accounts for the variation of these parameters and their effect on heat transfer and obtain a relationship of the form: $Nu \propto Re^a \varphi^b$. A multi-dimensional curve fit program was written in Matlab and produced the following correlations:

One rectangular opening:	$Nu = 0.775\,Re^{0.4935}\,\varphi^{0.4144}$
Two rectangular openings:	$Nu = 0.616\,Re^{0.4951}\,\varphi^{0.3964}$
Three rectangular openings:	$Nu = 1.219\,Re^{0.4455}\,\varphi^{0.2959}$
Two circular openings:	$Nu = 0.0305\,Re^{0.6639}\,\varphi^{0.2390}$

These correlations are applicable for $\theta = 30°$, $30° \leqslant \varphi \leqslant 90°$, and $2.71 \times 10^5 \leqslant Re \leqslant 1.62 \times 10^6$.

The jet angle (φ) should be entered in radians. The error resulting from using these correlations is 5.9% for one rectangular opening, 6.3% for two rectangular openings, 6.9% for three rectangular openings, and 8.5% for two circular openings. For more details on the error values, the reader is referred to [17].

For the detailed study case of three rectangular openings, eight hundred and eighty two simulations were performed, covering a range of Reynolds number, a range of inclined surface angle (θ), a range of issuing jet angles in the XY plane (φ) and the YZ plane (β). The angle (θ) can be alternatively replaced by a related dimensionless number, (H/D). For a hydraulic diameter (D) of 0.034 m, (H/D) would have the values of 2.12, 3.07, and 4.37 for inclined surface angles of 30°, 40°, and 50°; respectively. Numerical simulation results show that the average heat transfer coefficient increases as the H/D ratio decreases or as θ decreases. This is because the inclined surface experiences more of the potential core as the

Table 1
Comparison for the case with $Re = 8.12 \times 10^5$

Configuration	Angle in XY plane (φ deg)	Average h on the inclined surface (W/m^{2}K)	Nusselt number from simulations	Nusselt number from curve fit equation	Percentage change (absolute)
One rectangular opening	30	14.3005	467.42511	483.8935	3.52
	40	17.5056	572.18717	545.1605	4.72
	50	20.1095	657.2991	597.9762	9.03
	60	21.2312	693.96326	644.9063	7.07
	70	21.7959	712.42069	687.4472	3.51
	80	21.8386	713.81409	726.5595	1.79
	90	21.5917	705.7436	762.9021	8.10
Two rectangular openings	30	11.5352	377.0393	397.5676	5.44
	40	13.4427	439.38743	445.5913	1.41
	50	15.8489	518.03571	486.8014	6.03
	60	17.8232	582.56823	523.2862	10.18
	70	18.0650	590.47137	556.2589	5.79
	80	17.5096	572.31726	586.4959	2.48
	90	16.5856	542.11643	614.5282	13.36
Three rectangular openings	30	12.0720	394.58414	427.4753	8.34
	40	14.4300	471.65826	465.4578	1.31
	50	16.5646	541.42969	497.2285	8.16
	60	16.9467	553.91998	524.7902	5.26
	70	17.0875	558.52249	549.2819	1.65
	80	16.7062	546.05639	571.4196	4.64
	90	15.9330	520.78525	591.6858	13.61
Two circular openings	30	6.1676	201.59527	216.5936	7.44
	40	7.1138	232.51994	232.0097	0.22
	50	8.1684	266.99153	244.7189	8.34
	60	8.7309	285.37852	255.6183	10.43
	70	9.1577	299.3278	265.2114	11.40
	80	8.5725	280.20031	273.8119	2.28
	90	7.4979	245.07602	281.6292	14.92

H/D ratio decreases. In addition, at lower H/D ratios, the free jet region is small.

A multi-dimensional curve fit program written in Matlab produced the following relation:

$$Nu = 1.077 Re^{0.4624} (H/D)^{-0.0488} \varphi^{0.0956} \beta^{0.1712}$$

Or in terms of the angle, θ

$$Nu = 1.077 Re^{0.4624} \theta^{-0.0631} \varphi^{0.0956} \beta^{0.1712}$$

This correlation is applicable for

$$30 \leqslant \theta \leqslant 50, 30 \leqslant \varphi \leqslant 90,$$

$$35 \leqslant \beta \leqslant 90, 2.12 \leqslant \left(\frac{H}{D}\right) \leqslant 4.37,$$

and

$$2.71 \times 10^5 \leqslant Re \leqslant 1.62 \times 10^6$$

Nusselt and Reynolds numbers are based on the dimension of the inclined surface in the flow direction, H_1. When using the correlations, all angles (θ, φ and β) should be entered in radians. The overall error in using this correlation is ±7.4%. The above simulations were run on Sun Blade workstations with a CPU speed of 502 MHz and RAM of 768 Mbytes. The time to converge varies depending on the number of cells. For a case with 300,000 cells, the average time to converge was 6 h.

8. Conclusions

The increase in thickness of the boundary layer upstream of the jet impingement point on the inclined surface resulted in lesser heat transfer coefficients upstream when compared to those near the jet impingement point. Significant portion of the incoming fluid moved upward attaching the inclined surface, eventually moving downstream, thus causing recirculation downstream. The heat transfer in the stagnation zone created by jet impingement was found to be the maximum. For the comparative study, the overall heat transfer coefficient off the

inclined surface for the configuration with one rectangular opening was 16% more than that for the configuration with two rectangular openings, 21% more than that with three rectangular openings and 55% more than that with two circular openings. However, the mass flow rate for the two rectangular and circular openings is 50% of that for one rectangular opening and the mass flow rate for the three rectangular openings is 33% of that for one rectangular opening. Therefore, the configuration with three rectangular openings resulted in an average heat transfer value that is comparable to that of one rectangular opening but for a much lower flow rate. This is attributed to the wider spread and enhanced jet interactions on the surface for the case of multiple rectangular openings. Moreover, the temperature gradients on the inclined surface were inferred to be very high in the case of two circular openings compared to other cases. Numerically based correlations among Nu, Re, and φ were then generated for all configurations for predicting heat transfer on the inclined surface. For the detailed study for three rectangular openings, a numerically-based correlation among Nu, Re, (H/D) or θ, φ, and β was generated accounting for all affecting variables. The average heat transfer coefficient was observed to increase with decrease in H/D ratio as the amount of potential core in contact with the inclined surface decreased with increasing distance from the nozzle exit.

Acknowledgment

The authors would like to thank Professors Ruben Hayrapetyan and Joseph J. Salacuse of Kettering University for their insights on generating curve fits.

References

[1] H. Martin, Heat and mass transfer between impinging gas jest and solid surfacesAdvances in Heat Transfer, vol. 13, Academic Press, New York, 1977, pp. 1–60.
[2] S.J. Downs, E.H. James, Jet impingement heat transfer-a literature survey, ASME paper no. 87-HT-35, 1987.
[3] S. Polat, B. Huang, A.S. Mujumdar, W.J.M. Douglas, Numerical flow and heat transfer under impinging jets: a review, Ann. Rev. Numer. Fluid Mech. Heat Transfer 2 (1989) 157–197.
[4] R. Viskanta, Heat transfer to impinging isothermal gas and flame jets, Exp. Therm. Fluid Sci. 6 (1993) 111–134.
[5] E.M. Sparrow, B.J. Lovell, Heat transfer characteristics of an obliquely impinging circular jet, ASME J. Heat Transfer 102 (2) (1980) 202–209.
[6] R.J. Goldstein, M.E. Franchett, Heat transfer from a flat surface to an oblique impinging jet, ASME J. Heat Transfer 110 (1988) 84–90.
[7] A.K. Mohanty, A.A. Tawfek, Heat transfer due to a round jet impinging normal to a flat surface, Int. J. Heat Mass Transfer 36 (6) (1993) 1639–1647.
[8] S.J. Lee, J.H. Lee, D.H. Lee, Local heat transfer measurements from an elliptic jet impinging on a flat plate using liquid crystal, Int. J. Heat Mass Transfer 37 (6) (1994) 967–979.
[9] L. Huang, M.S. El-Genk, Heat transfer of an impinging jet on a flat surface, Int. J. Heat Mass Transfer 37 (13) (1994) 1915–1923.
[10] A. Bernard, L.-E. Brizzi, J.-L. Bousgarbies, Study of several jets impinging on a plane wall: Visualizations and laser velocimetry investigations, ASME J. Fluids Eng. 121 (1999) 808–812.
[11] J.C. Bailey, R.S. Bunker, Local heat transfer and flow distributions for impinging jet arrays of dense and sparse extent, ASME paper no. GT-2002-30473, 2002.
[12] S. Roy, K. Nasr, P. Patel, B. AbdulNour, An experimental and numerical study of heat transfer off an inclined surface subject to an impinging airflow, Int. J. Heat Mass Transfer 45 (2002) 1615–1629.
[13] S. Roy, P. Patel, Study of heat transfer for a pair of rectangular jets impinging on an inclined surface, Int. J. Heat Mass Transfer 46 (2003) 411–425.
[14] FLUENT 5 User's guide, Fluent Inc., Lebanon, NH.
[15] B.E. Launder, D.B. Spalding, The numerical computation of turbulent flows, Comput. Methods Appl. Mech. Eng. 3 (1974) 269–289.
[16] GAMBIT 1 User's guide, Fluent Inc., Lebanon, NH.
[17] S. Rasipuram, Flow patterns and heat transfer off an inclined surface subject to airflow, Masters thesis, Kettering University, Flint, MI, 2003.